EDGES MEMO #289

MASSACHUSETTS INSTITUTE OF TECHNOLOGY
HAYSTACK OBSERVATORY
WESTFORD, MASSACHUSETTS 01886

October 17, 2018

Telephone: 617-715-5533
Fax: 617-715-0590

To: EDGES Group

From: Alan E.E. Rogers

Subject: Considerations for placing the electronics on the antenna

Powerful PCs like the Nuvo-7000 series are now available in a small enough form factor to become part of the antenna. Figure 1 shows an antenna in which the panels have been made into boxes with dimensions of 73.4×95.3×12 cm in length × width × height. The Nuvo PC is 22.5×24.0×11.05 cm and would take up only about 10% of the area of the box. In addition, the Nuvo includes an internal PCIe slot for the Signatec PX14400 ADC card. A vector network analyzer, like the keysight Streamline P9370A would occupy 33.5×17.6×4.9 cm. Figure 2 shows a sketch of the component placement with the box which is part of the antenna and Figure 3 shows a block diagram of the receiver which includes the added switches along with built in hot, ambient loads open and shorted cables and VNA calibration for automated calibration of the receiver and measurement of the antenna S11.

Sufficient isolation of the RFI from a PC under the antenna was demonstrated by the array of antennas used to measure the spectra from the Deuterium in the Galaxy (Rogers, Dudevoir and Bania, ApJ. 133:1625-1632 2007). In this array more than about 192 dB of isolation between the inside of the receiver in the box under the dipole antenna was obtained through the use of a closed box with screws spaced a twentieth of a wavelength apart on the box cover along with a fiber optic connection to the outside and double filtering of the a.c. power as it enters the receiver box.

Simulations of the effects of the boxes on the beam chromaticity using FEKO show that there is very little change compared with midband blade provided the height center of the boxes is the same as the panel height of the midband antenna with same dimensions as those given in memo #267. The average residual to a 5-term polynomial from 50-100 MHz for 2 hour blocks of GHA is 20 mK and 30 mK for latitudes of 31 and -27 degrees respectively for the antenna on the 30×30 m ground plane. Simulations of the the effect of S11 errorare also similar for the midband blade antenna and an antenna in which the panels become boxes with 12 cm height. However, the increased thickness of the panels to 12 cm improves the S11 below 55 MHz so that at 40 MHz the S11 is -0.4 dB compared with -0.2 dB for the blade.

Placing the electronics in the antenna eliminates the need for the balun which has a loss of about 0.02 dB (see memo #273).

In addition, the elimination of the balun reduces the delay in the antenna S11 from 24 to 17 ns.

Simulations of the S11 accuracy needed for the measurement of the antenna and LNA were made by generating spectra using the foreground plus the absorption profile reported in Nature and processing using a 10 term polynomial fit to the ground plane. The sensitivity to errors in S11 were tested by applying an offset in S11 magnitude and delay is given in in Table 1.

LNA offset		Antenna offsets		Freq. range	#terms
ps	dB	ps	dB	MHz	
500	1.0	500	0.1	55-100	5
10	0.1	10	0.005	41-100	5
100	0.5	100	0.05	41-100	8

Table 1 sensitivity thresholds for detection of absorption due to error in S11 measurement.

The criteria for the threshold were based on a detection of the absorption as the best fit from a grid search that covers a center frequency range of 60 to 90 MHz width 5 to 40 MHz and with τ=7. No noise was added and the results were found to be largely independent of the size of the ground plane from 2×2 m to infinite PEC although intermediate sized ground planes have large beam chromaticity. These simulations show that very accurate S11 measurements are needed to cover 41-100 MHz when only 5 polynomial terms are used to model the systematics alone. In addition, this applies even when the antenna becomes electrically small.

The automated internal calibration system will use high quality stable silicon dioxide cables to provide very stable paths between the receiver input reference plane and the other inputs of the 8-position switch to the LNA and to the VNA. In addition, a very stable path is provided between the VNA and the LNA to be able to measure the LNA S11. The full S-parameters of these 17 paths will be measured in the laboratory using a combination of the internal VNA and a separate external VNA. These S-parameters will be used to enable the S11 and losses to be referred to the reference plane of the input of the receiver using the relationships given in memo 132. For all the S11 measurements this is the standard de-embedding and embedding of networks. The correction of the spectra taken with internal hot load as well as ambient load and open and shorted cables require the measurement of the temperatures of the device and the temperature and loss of the path in addition to the S-parameters of the paths involved using the algorithms summarized in memo 132 and given in Monsalve et al 2017.

In simple terms the function that inverts the 3-position switched spectra is used to invert the spectra using the actual path S-parameters and LNA S11 at the location on the devices are then multiplied by the ratio of the spectra computed for the receiver reference location to that computed for the actual location. For this the expression for the power in memo #132 is augmented with loss corrections for the noise wave amplitudes

$$P = \left[\left(T_{sky} L + T_{amb} \left(1 - L \right) \right) \left(1 - \left| \Gamma_a \right|^2 \right) \right] \left| F \right|^2$$
$$+ \left[T_c \, \mathrm{Re} \left(\Gamma_a F \right) + T_s \, \mathrm{Im} \left(\Gamma_a F \right) \right] L_2$$
$$+ \left[T_u L_2 + T_{amb} \left(1 - L_2 \right) \right] \left| \Gamma_a \right|^2 \left| F \right|^2$$

where L2 is the loss of the path to the LNA. An alternative approach is to define the reference plane to be at the input of the LNA and calculate Γ_a at this reference plane for antenna as well as hot, ambient loads and open and shorted cables.

Mechanical switches with short cables between the switches and the LNA and VNA are used to provide low loss paths and good shielding. Apart from the LNA and noise sources commercially available modules with connectors will be used for best isolation between modules and to minimize the need to develop many new PC boards. Also having individually shielded modules will minimize cross-coupling and any feedback which could change with switch positions and effect the calibration accuracy. It may be necessary to enclose the PC in a box within the box to obtain sufficient shielding from the antenna. About 160 dB is needed to reduce the feedback into the antenna to have an effect below 1 mK. The shielding effectiveness in terms of power radiated by 1 foot of solid shield cable is about 200 dB but radiation from the connectors is more significant and clip-on ferrites will be used to minimize common mode effects like that described in memo #284. In addition, only 3.5 mm connectors will be used instead of the older standard and poorly define SMA connectors (see memo #270). Further some absorbing material will also be placed in the box to suppress resonance effects.

Air will be circulated within the box to provide temperature control of the LNA using thermoelectric modules to exchange heat with the air via conduction to the antenna box. The details being similar to that described in memo 123. The antenna boxes will be plated with Goldstone #6 titanium dioxide paint to

limit the box temperature to prevent excessive temperatures due to solar radiation. The pc is specified to 70˚C but the calculations show it should be possible to keep the temperature below 60 ˚C. The pc will have a MezIO which provides 16 channel of isolated digital I/O to control the mechanical switches. Temperatures will be monitored at up to 8 locations using an 8-channel Omega USB module with thermistor probes.

The key components are

Nuvo-7000DE with

2x GigE LAN ports

Size: 240 mm (W) × 225 mm (D) × 110.5 mm (H)

4 × USB 3.1 Gen2 and 4 × USB 3.1 Gen1

2× software-programmable RS-232/442/485 ports (COM1/COM2)

2× RS-232 ports (COM3/COM4)

1× VGA connector 1920 x 1200 resolution

DVI-D connector supporting 1920 × 1200 resolution

Display Port connector, supporting 4096 × 2304 resolution

MezIO-D230 16-ch isolated digital I/O which can be used under Linux.

1 PCIe slot for PX14400A and 1 PCIe slot for Ethernet via fiber

Current EDGES-2 front and backend re-packaged without bias-tees using MezIO-D230 to flexibly control latching SP8T Teledyne CCR-395 switch switches to +12V

Laird DA-075-12-02 with Oven Industries 5R7 RS232 controller

Omega USB-TEMP for 8 temperature probes and 8 more digital I/O if needed

Keysight P9370A USB VNA

Simulations of EDGES-3 performance

More detail of the effects of systematics are including a comparison with midband are given in Table 2

Source of error	rms K	# terms	rms before (mK)	rms after (mK)
No beam correction	6.95	6	99	43
30 ps error in S11	0.29	5	115	41
0.002 dB error in S11	1.09	5	160	33
No balun loss	3.9	5	115	31
0.002 dB error in S11	2.4	5	203	65

Table 2 Effect of systematic error in simulated search for absorption.

Table 2 given the results of a simulation over a range of 45-130 MHz in which an absorption signature from the Nature paper is added to a foreground with spectral index of -2.55 and 1697 K at 75 MHz. The first column lists the change made to the simulated data, the second column the rms change in the spectrum, the third column givens the minimum number of terms of a quasi physical polynomial needed to obtain the absorption signature within the Nature errors without ambiguity in a grid search over frequency and width for a constant flattening of τ =7. The fourth and fifth columns give the rms of the best fit before and after adding an absorption to the fit.

The second to last entry shows effect of the midband balun loss, which will not be present in EDGES-3, can be significant. The last entry shows, in comparison with the third entry, that the wider frequency coverage of reflection coefficient reduces the effect of error in the measurement of the antenna S11 by a factor of about two. The effects of error in S11 phase and beam correction, which was made for the beam at GHA = 12 hours on the 30×30 m ground plane is about the same for the EDGES-3 and the current midband.

Simulations of the effect of the elimination of the balun delay

The results of a simulation using the S11 from mid-rcv1-20180527/2018_147_16_52_34 for antenna S11 and subtracting 6 nanoseconds of balun delay are given in Table 3.

# terms of EDGES polynomial – rms residuals in mK						
Case	1	2	3	4	5	6
A	18150	849	319	170	150	47
B	17524	723	415	173	45	36
C	16889	972	443	163	129	34
D	16985	450	395	124	39	34

Table 3.

A simulated data at GHA = 12 50 – 100 MHz processed with 100 ps change in antenna A

B same as A but with 6 ns subtracted from antenna S11 to account for the removal of the balun

C and D for 100 ps change in LNA S11

These results scale so that for 10 ps S11 error they are a factor of 10 smaller.

	LINPHYS	POLY	LINPOLY	LOGLOG
A	146	150	150	183
B	50	75	45	98
C	125	130	129	175
D	43	62	39	74

Table 4. rms residuals in mK for 5-terms using different functions defined in ASU memo #122.

The effects of removing the 6 ns delay is very small for other systematics like error in the antenna or LNA S11 magnitude. In summary not having a balun avoids systematics due to errors in the balun loss and reduces the effects of errors in the measurement antenna and LNA S11 phase due to the added fine structure in the antenna S11 measured at the receiver which arises due to the delay in the balun.

In summary, the elimination of a blun delay makes a substantial reduction of the effects of S11 phase error when 5 terms but not as much when 6 or more terms are removed.

Memos 186, 204, 251, 263, 265, 289, 290 have information on antennas and ground planes. A summary of what is found

1] Effects of beam chromaticity with antenna on infinite PEC ground plane are the same for a dipole, the blade and the bladebox and increase for a length and height of more than 1/3 wavelength and ¼ wavelength respectively at the high end of the frequency band.
2] The lowest S11 over a 2:1 range requires going to about 1/3 wavelength in length and ¼ wavelength in height.

3] The added beam chromaticity and ground loss contributed by a real ground plane is about the same for a dipole, the blade and the bladebox.
4] The ground plane has to be larger than about 5×5 wavelengths or smaller than about 1/3×1/3 wavelength at the low end to approach the beam chromaticity on an infinite PEC ground plane.
5] FEKO provides a good ground loss estimate (see memo 290) provided it is smoothed with a 4-term polynomial to filter out inaccuracies in computation.

When deployed at the MRO EDGES-3 will use the 30×30 m ground plane in order to give the best performance needed to further explore the details of the absorption including a more accurate flattening profile and extensions to higher and lower frequencies. EDGES-3 will be better suited to a short deployment at other sites like the Catlow Valley region of Oregon which was shown in 2009 to have a low level of RFI comparable to the MRO (see memo 50). For such a deployment a large ground plane can be constructed using parallel wires which can be easily placed on the ground as in Figure 3 of memo #75. A 30×8 m ground plane with wire spacing of 62.5 cm using 6000 ft of #10 wire is low cost and can be deployed in a few hours. FEKO simulations show that the ground loss is under 1% from 50 to 140 MHz.

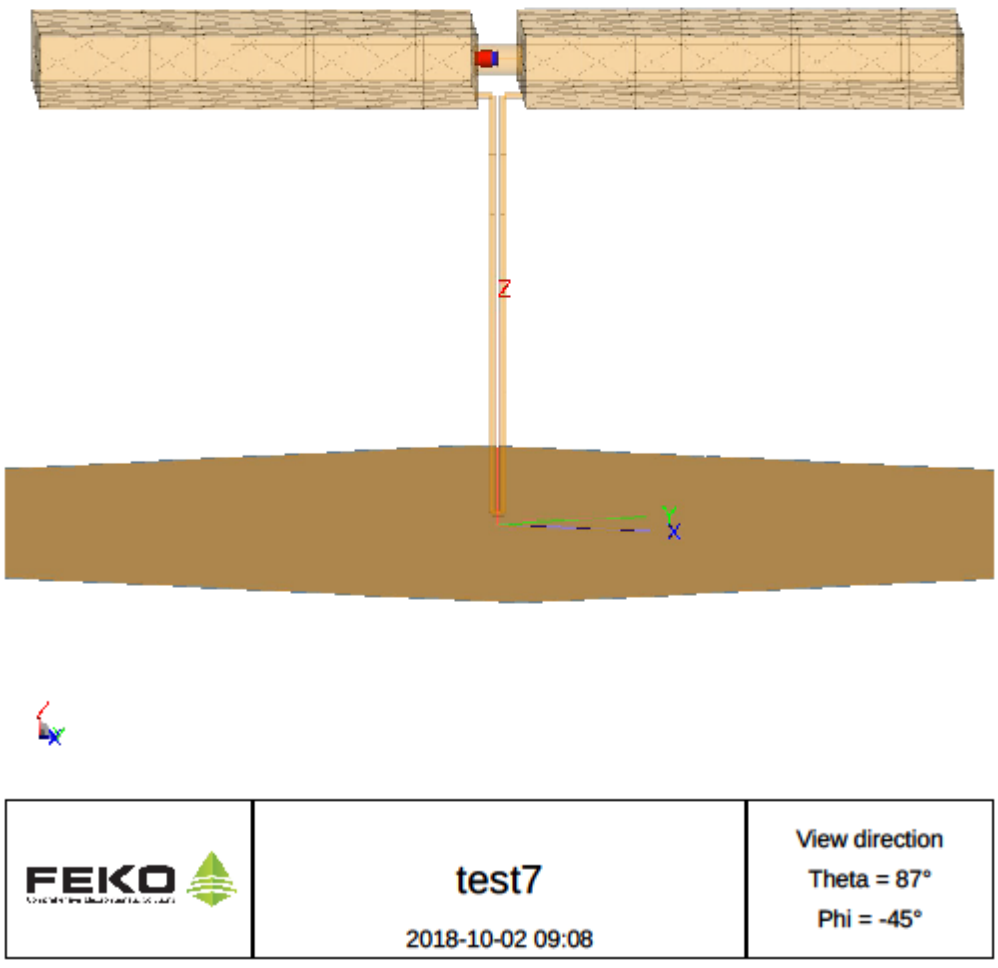

Figure 1. FEKO model of blade antenna with panels made into boxes.

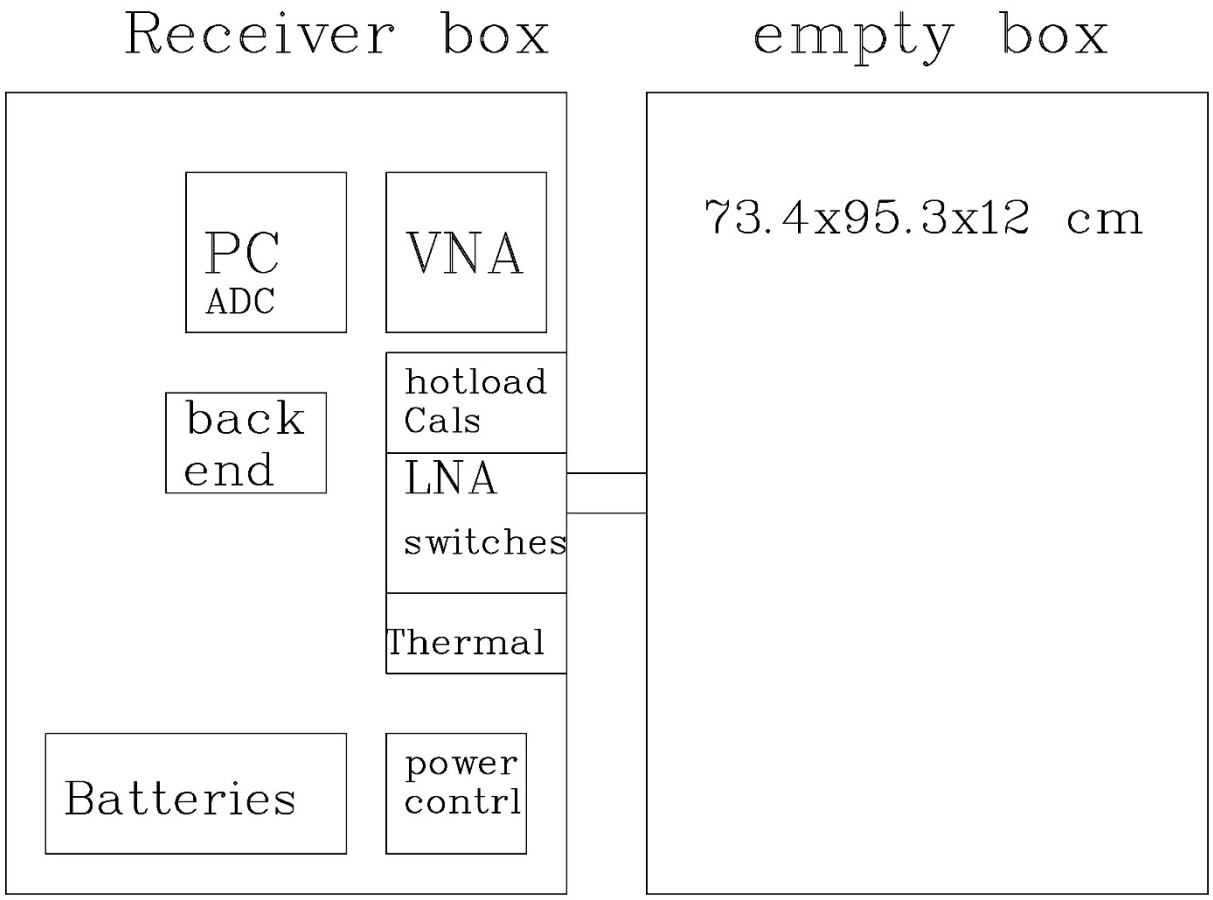

Figure 2. Sketch of proposed layout of receiver and VNA.

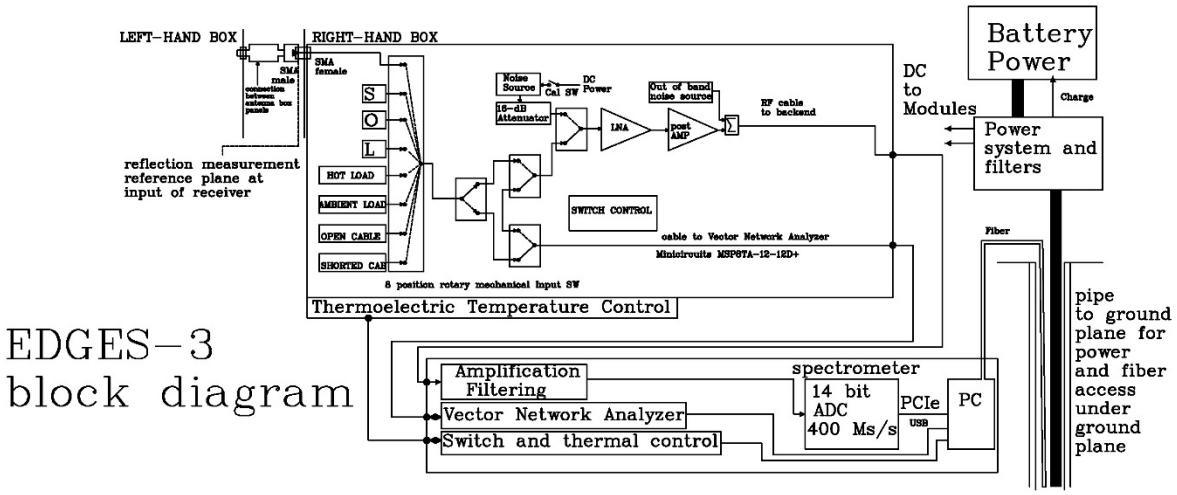

Figure 3. Block diagram of modules for receivers plus S11 measurement system, thermal control and switching for automated calibration of the receiver.